Synthesis of a Novel Polymer- Iron (III) Complex and Study of Its Anticancer Properties on A375 Melanoma Cell Line

Elham Neisi and Siavash Hasanvandi *

Posted Date: 31 August 2023

doi: 10.20944/preprints202308.2171.v1

Keywords: 1-(2-((3-amino-2-hydroxypropyl)amino)ethyl)-1'-ethyl-[4,4'-bipyridine]-1,1'-diium; Iron Polymer-Complex; MTT; A375 cells.

Article

Synthesis of a Novel Polymer- Iron (III) Complex and Study of Its Anticancer Properties on A375 Melanoma Cell Line

Elham Neisi and Siavash Hasanvandi *

Department of Chemistry, Lorestan University, Lorestan, Iran 1; elham.neisi@yahoo.com
* Correspondence: S.hasanvandi@gmail.com; Tel.: +98-6633120618

Abstract: In the present study, linear novel polymer poly(1-(2-((3-amino-2-hydroxypropyl)amino)ethyl)-1'-ethyl-[4,4'-bipyridine]-1,1'-di-ium) (poly(AHAEBD)) and its complex with iron (III) ([Fe(poly(AHAEBD)$_2$].Na$_3$) were synthesized and then their anticancer effects on A375 human malignant melanoma cells line were evaluated. The structure of the synthesized compounds was confirmed using Fourier transform infrared spectroscopy (FT-IR), nuclear magnetic resonance spectroscopy (^{1}HNMR), field emission scanning electron microscopy (FE-SEM), X-ray energy diffraction analysis (EDS) and gel permeation chromatography (GPC). Also, the cytotoxicity of cisplatin as a reference, on A375 melanoma cell line was tested. The IC$_{50}$ of polymer-complex [Fe(poly(AHAEBD)$_2$].Na$_3$ (0.71 µg/mL), cisplatin (4.58 µg/mL) and poly(AHAEBD) (1.73 µg/mL) were obtained. Our results revealed that the polymer-complex [Fe(poly(AHAEBD)$_2$].Na$_3$ exhibited better performance compared to cisplatin. Furthermore, the coordination with iron (III) enhanced the cytotoxicity levels of poly(AHAEBD). According to these findings, the synthesized polymer-complex demonstrates remarkable potential as an anti-cancer agent. This study could provide the basis for future research focused on employing this new polymer-complex for in vivo testing, highlighting its potential for therapeutic applications.

Keywords: 1-(2-((3-amino-2-hydroxypropyl)amino)ethyl)-1'-ethyl-[4,4'-bipyridine]-1,1'-diium; iron polymer-complex; MTT; A375 cells

1. Introduction

Melanoma, a type of skin cancer that originates in melanocytes, the cells responsible for producing the pigment melanin is a topic of increasing concern in the field of oncology [1]. With its potential to metastasize rapidly, melanoma poses a significant threat to patients' health and survival. Chemotherapy stands as one of the most common methods in the treatment of skin cancer [2]. Metal-based compounds have held a significant role in chemotherapy research for an extended period [3]. Meanwhile, iron complexes are promising alternatives to conventional platinum-based chemotherapy due to their wide range of reactions and targeting different biological systems [4]. Iron assumes a pivotal role in programmed cell death, and many studies have been conducted on iron compounds to develop potential strategies for tumor therapy [5]. The rapid multiplication of malignant cancer cells is significantly influenced by the disruption of iron homeostasis. This dysregulation commonly occurs during the stages of growth and proliferation, driven by the heightened iron demands of these cells. Consequently, compounds incorporating iron hold the capability to efficiently entrance the cells, effectively stopping the growth of cancerous tumors, and ultimately inducing the demise of cancer cells [6,7]. Moreover, elevating the cellular iron dose triggers an upsurge in radical species like hydroxyl radicals. These radicals launch an attack on the nucleic acid sequences within DNA, consequently disrupting the life cycle of cancer cells and inhibiting their proliferation [8,9].

Polymer-metal complexes embody featuring a polymer backbone coupled with a metal ion or metal nanoparticles, linked via coordination bonds. Renowned for their distinctive physical and

chemical attributes, these complexes have gained widespread utility across diverse fields, including pharmaceuticals, biomedicine, and biological research [10–12]. Within the pharmaceutical domain, polymer-metal complexes have emerged as an important strategy in novel drug development. Using metal coordination chemistry, these complexes can be tailored to precisely target disease-causing biomolecules, yielding substantial therapeutic outcomes [13].

Beyond pharmaceuticals, polymer-metal complexes have demonstrated important applications in the realm of biomedicine. For example, polymer-gold complexes have been investigated for their use as nanocarriers in targeted drug delivery due to their ability to selectively accumulate in tumor tissues [14]. Also, in medical imaging, polymer-iron complexes function as contrast agents in magnetic resonance imaging (MRI), contributing to enhanced diagnostic capabilities [15]. some research has been conducted to explore the anti-cancer impact of polymer-complexes containing diverse metals [16,17], including the investigation of the anti-cancer effect of polymer-complexes of iron and zinc on cancer cells [18].

In recent years, substantial focus has been directed towards viologen compounds, specifically bipyridinium, attributed to their notable charge density and integral involvement in redox reactions [19]. Constructing linear polymers based on ionic compounds like viologen, characterized by alternating functional groups such as amine and hydroxy, offers a pathway to create complex polymers with many metals. Due to their positive charge, polycationic compounds have attracted a lot of attention in biological systems [20]. Synthesis a linear polymer that coordinates with metals via various functional groups is an innovative approach for creating anti-cancer polymer compounds. The polymer's positive charge enhances its applications by improving water solubility and facilitating binding to multiple metals. This charge also promotes stronger binding with biological macromolecules [21,22].

In the present work, poly(1-(2-aminoethyl)-'1-(2-((2-hydroxypropyl)amino)ethyl)-[4,'4-bipyridine]-1,'1-dioe) (poly(AHAEBD)) was synthesized and its iron polymer-complex was used to investigate the effect on A375 human malignant melanoma cells. New design in poly(AHAEBD) structure, high solubility, ability to form complex with ions such as iron and high cytotoxicity for cancer cells are distinguishing features of this study.

2. Materials and Methods

2.1. Materials

The following chemicals were used in the study: 4,4'-bipyridine (4,4'-BP, 98%, Sigma-Aldrich), 2-bromoethylamine hydrobromide (2-BEA, 99%, Merck), ethanol, dimethylsulfoxid (DMSO), ethyl acetate, epichlorohydrine (ECH) and acetone were of high purity (>99%, Merck), $Fe(NO_3)_3.9H_2O$ and NaPF6 (Sigma-Aldrich). DMEM (Dulbecco's modified Eagle's medium), 3-(4,5-dimethylthiazol-2-yl)-2,5-diphenyltetrazolium bromide (MTT) and cisplatin were obtained from Sigma-Aldrich and A375 human malignant melanoma cells line was obtained from Pasteur Institute of Iran. Other solvents and materials were obtained from Merck and used without further purification.

2.2. Characterization

Fourier-transform infrared (FT-IR) spectra were recorded on a SHIMADZU 8400 spectrophotometer using KBr pellets (4000-400 cm^{-1}). The field emission scanning electron microscope (FE-SEM) used in this study was the TESCAN MIRA III, (Czech Republic) and energy dispersive X-ray analysis (EDS) was carried out using SAMx EDS (France). ^1H nuclear magnetic resonance (^1HNMR) spectra were recorded using a VARIAN NMR spectrometer (Inova 500MHz) in D_2O. The molecular weight of the polymer was determined using permeation gel chromatography (GPC, Agilent Instrument).

Preprints (www.preprints.org) | NOT PEER-REVIEWED | Posted: 31 August 2023 doi:10.20944/preprints202308.2171.v1

2.3. Synthesis procedures

2.3.1. Synthesis of 1,1'-bis(2-aminoethyl)-[4,4'-bipyridine]-1,1'-diium (BABD)

To a 10 mL solution of anhydrous ethanol, 4,4'-BP (0.2 g, 1.28 mmol) and 2-BEA (0.525 g, 2.56 mmol) were added, and the mixture was refluxed at 80 °C for 48 h. After filtration and washing with ethanol and acetone, 0.63 g of BAED was obtained with an 87% yield. EDS (At%) elemental analysis results, ($C_{14}N_4Br_4H_{20}$): C (63.41%), N (18.42%) and Br (18.14%).

2.3.2. Synthesis of poly(1-(2-((3-amino-2-hydroxypropyl)amino)ethyl)-1'-ethyl-[4,4'-bipyridine]-1,1'-di-ium) (poly(AHAEBD))

1.13 g of BABD (2 mmol) and 3.5 mL of ECH (about 4.2 mmol) were added to 10 mL of DMSO and refluxed at 70 °C for 4 h, then 5 mL of ethyl acetate was added to the above solution to precipitate the poly(AHAEBD). Subsequently, the synthesized compound was washed several times using ethyl acetate. The final product displayed a reaction yield of 83%. The EDS elemental analysis showed the following composition, ($C_{17}N_4OCl_2$): C (70.13%), N (15.90%), Cl (9.03%) and O (4.94%).

2.3.3. Synthesis of polymer-complex [Fe(poly(AHAEBD)$_2$].Na$_3$

In a 15 mL deionized water, 0.75 g of poly(AHAEBD) (2 mmol) and 0.41 g of $Fe(NO_3)_3.9H_2O$ (1 mmol) were added and stirred for 48 h at 40 °C. Then, 0.67 g of $NaPF_6$ (4 mmol) was introduced to the solution, resulting in the formation of a pale-yellow precipitate. The obtained precipitate was filtered and subjected to multiple washes using deionized water (DI) and acetone, yielding a reaction efficiency of 79%. The EDS elemental analysis showed the following composition: ($C_{34}N_8O_2P_4F_{24}Na_3Fe$): C (42.08%), N (10.02%), O (3.66%), P (4.94%), F (33.23%), Na (4.12%), and Fe (1.95%). The synthesis route of [Fe(poly(AHAEBD)$_2$)].Na$_3$ is illustrated in Figure 1.

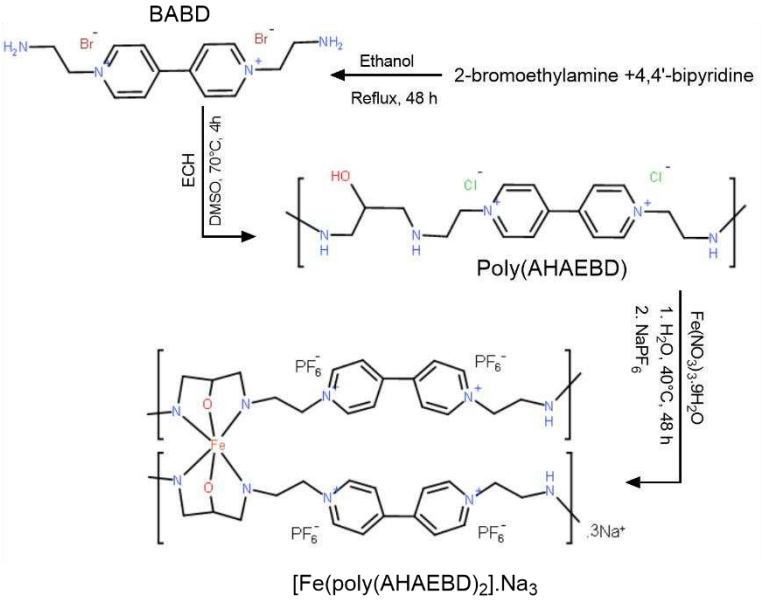

Figure 1. Synthesis route of BABD, poly(AHAEBD) and [Fe(poly(AHAEBD)$_2$].Na$_3$.

2.4. Cell culture

A375 human malignant melanoma CELLS were cultured in DMEM containing 10% fetal bovine serum (FBS) and 1% penicillin/streptomycin (PS) in a humid environment (95% humidity) with 5% CO_2 at 37 °C. The viable cells were counted using a hemocytometer, based on their ability to exclude trypan blue. Drug treatment was initiated after a 4-hour incubation period. Stock solutions (20 μg/mL in DMSO) of [Fe(poly(AHAEBD)$_2$].Na$_3$ and poly(AHAEBD), and cisplatin (40 μg/mL in deionized

Preprints (www.preprints.org) | NOT PEER-REVIEWED | Posted: 31 August 2023 doi:10.20944/preprints202308.2171.v1

water) were prepared and subsequently diluted with the culture medium to achieve the desired concentrations whenever needed [23–25].

3. Results and discussion

3.1. FT-IR Spectroscopy

The FT-IR spectra of BABD, poly(AHAEBD), and [Fe(poly(AHAEBD)$_2$)].Na$_3$ compounds are depicted in Figure 2. In the BABD spectrum, absorption bands at 3464 and 3526 cm^{-1} correspond to N-H stretching vibrations, while bands at 1601 and 1643 cm^{-1} related to C=N and C=C stretching vibrations, respectively [26]. Similar absorption bands at 1601 and 1643 cm^{-1} are also observed in the spectrum of poly(AHAEBD). Both BABD and poly(AHAEBD) display aliphatic and aromatic C-H regions in the range of 2950-12850 cm^{-1} and 3020 cm^{-1} respectively. A broad absorption band in the 3200 to 3400 cm^{-1} is indicative of the hydroxy group in the poly(AHAEBD). The absorption band at 1558 cm^{-1} in both BABD and poly(AHAEBD) signifies the N-H bending frequency [27]. Additionally, the absorption band at 1407 cm^{-1} corresponds to the C-O stretching frequency [28].

In [Fe(poly(AHAEBD)$_2$)].Na$_3$, the frequencies aligned with C=N and C=C stretching vibrations are evident at 1604 and 1639 cm^{-1} [29]. The disappearance of the absorption band of N-H bending vibration and the absence of the absorption band associated with the hydroxy group indicate the hydrogen removal from the hydroxy and amine groups of poly(AHAEBD), signifying their coordination to iron (III).

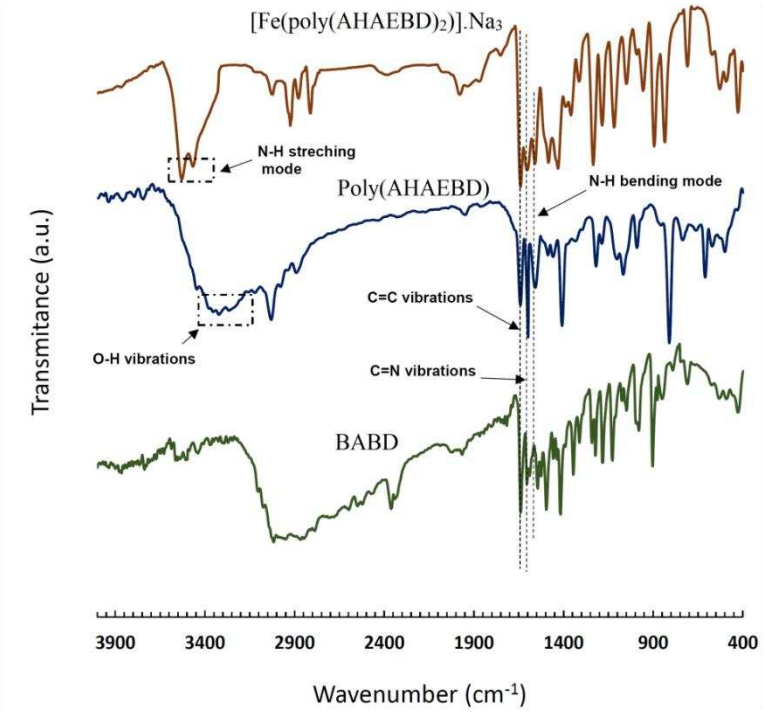

Figure 2. The FT-IR spectra of BABD, poly(AHAEBD) and [Fe(poly(AHAEBD)$_2$].Na$_3$.

3.2. ^{1}HNMR study

The Figure 3 illustrates the ^{1}HNMR spectra of BABD, poly(AHAEBD), and [Fe(poly(AHAEBD)$_2$)].Na$_3$ compounds. Within the poly(AHAEBD) compound, three distinct hydrogen types are identifiable. These including the hydrogen of the hydroxy group (at 9.94 ppm, associated with carbon number 1), along with hydrogens attached to carbon numbers 5 and 6 (with chemical shifts of 4.89 ppm and 4.46 ppm, respectively). These two hydrogens have been incorporated into the BABD spectrum as a result of the reaction with ECH. In the [Fe(poly(AHAEBD)$_2$)].Na$_3$ spectrum, the absence of the hydrogen associated with the hydroxy group

Preprints (www.preprints.org) | NOT PEER-REVIEWED | Posted: 31 August 2023 doi:10.20944/preprints202308.2171.v1

and changes in the chemical shift of hydrogens signifies the interaction of the iron ion with the poly(AHAEBD) [30].

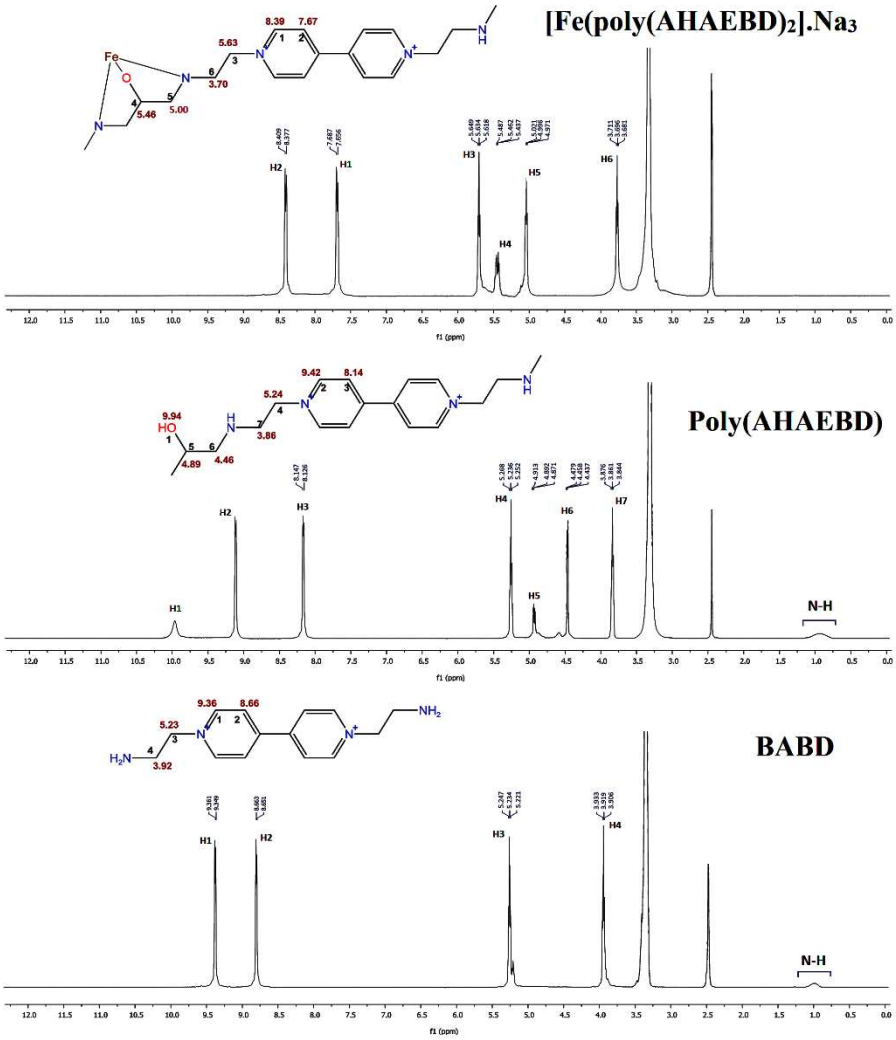

Figure 3. 500 MHz ^{1}H NMR spectrum of BABD, poly(AHAEBD) and [Fe(poly(AHAEBD)$_2$].Na$_3$ obtained in DMSO-d$_6$ at 298 K.

3.3. GPC analysis of poly(AHAEBD)

The poly(AHAEBD) exhibits remarkable water solubility owing to its polycationic nature. This characteristic makes it an ideal candidate for reactions in aqueous medium. Also, its distinctive arrangement of alternating amine and hydroxy groups renders it proficient in forming effective coordination bonds with various metals, including iron (III). For GPC analysis, a sample was prepared using DI at a concentration of 1 g/L. The analysis was conducted utilizing a water eluent phase and employing a differential refractometer (DRI) as detector. The chromatogram was shown in Figure 4. The GPC analysis unveiled the weight-average molecular weight (Mw) at 21290 g/mol, the number-average molecular weight (Mn) at 10138 g/mol, and a polydispersity index (PDI) of 2.1 for the poly(AHAEBD) polymer.

Preprints (www.preprints.org) | NOT PEER-REVIEWED | Posted: 31 August 2023 doi:10.20944/preprints202308.2171.v1

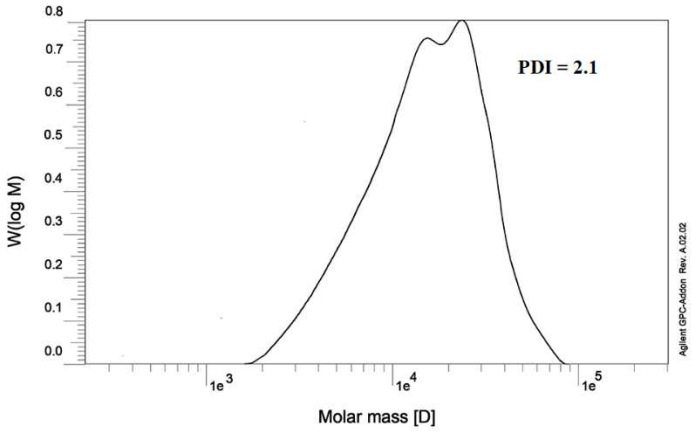

Figure 4. Molecular weight distribution of poly(AHAEBD) analyzed by GPC (with eluent phase of water).

3.4. EDS and FE-SEM analysis

Figure 5 represents FE-SEM images of poly(AHAEBD) and the [Fe(poly(AHAEBD)$_2$)].Na$_3$ complex-polymer. Sample preparation for FE-SEM analysis included sonicating a 5 mg/mL aqueous suspension of [Fe(poly(AHAEBD)$_2$)].Na$_3$ and an aqueous solution of poly(AHAEBD) for 5 min in an ultrasonic bath. Then, the prepared samples were dried onto a silicon wafer substrate. In the FE-SEM image of, poly(AHAEBD) (Figure 5a) an abundance of accumulated spherical structures can be seen, while the FE-SEM of [Fe(poly(AHAEBD)$_2$].Na$_3$ (Figure 5d) reveals faceted structures characterized by sharper edges. Elemental distribution maps in Figure 5b,e illustrate iron distribution for poly(AHAEBD) and [Fe(poly(AHAEBD)$_2$)].Na$_3$, respectively. Notably, the absence of iron in Figure 5b and the distinct distribution of iron elements in Figure 5e are evident. Figure 5c,f also display the EDS spectra of poly(AHAEBD) and [Fe(poly(AHAEBD)$_2$].Na$_3$, respectively. As shown, the spectrum of [Fe(poly(AHAEBD)$_2$].Na$_3$ clearly reveals the presence of iron, whereas the spectrum of poly(AHAEBD) shows no detectable iron content. Alongside with other analyses, these findings emphasize the alterations in structure and coordination of the poly(AHAEBD) compound with iron ions.

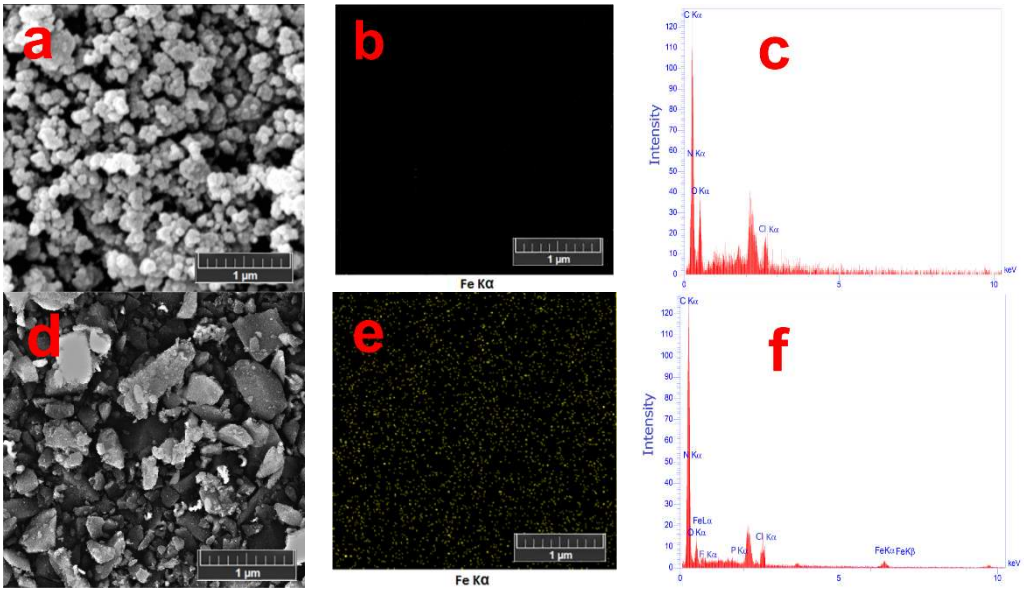

Figure 5. FE-SEM images of a) poly(AHAEBD) and e) [Fe(poly(AHAEBD)$_2$].Na$_3$, EDS mapping images of b) poly(AHAEBD) and e) [Fe(poly(AHAEBD)$_2$].Na$_3$, and EDS spectra of c) poly(AHAEBD) and f) [Fe(poly(AHAEBD)$_2$].Na$_3$.

Preprints (www.preprints.org) | NOT PEER-REVIEWED | Posted: 31 August 2023 doi:10.20944/preprints202308.2171.v1

3.5. Cytotoxicity analysis

The cytotoxic properties of [Fe(poly(AHAEBD)$_2$)].Na$_3$, poly(AHAEBD), and cisplatin (as a reference) were evaluated on A375 cancer cells using the MTT method. Table 1 presents the IC$_{50}$ values resulting from a 24 h treatment of these compounds on A375 cancer cells in a culture medium. Cisplatin exhibited IC$_{50}$ value of 4.58 µg/mL [31], while [Fe(poly(AHAEBD)$_2$)].Na$_3$ and poly(AHAEBD) displayed IC$_{50}$ values of 0.71 µg/mL and 1.73 µg/mL, respectively.

Table 1. IC$_{50}$ ± SD (µg/mL) values for [Fe(poly(AHAEBD)$_2$].Na$_3$, poly(AHAEBD) and cisplatin on A375 cancer cell line.

IC$_{50}$ ± SD (µg/mL)	Compound
0.71 ± 0.006	[Fe(poly(AHAEBD)$_2$].Na$_3$
1.73 ± 0.011	Poly(AHAEBD)
4.58 ± 0.032	Cis-platin

Figure 6 illustrates the cell viability percentages under six treatment concentrations of [Fe(poly(AHAEBD)$_2$)].Na$_3$, poly(AHAEBD), and cisplatin. It is evident from the results that the polymer-complex [Fe(poly(AHAEBD)$_2$)].Na$_3$ exhibits a significantly lower IC$_{50}$ value compared to both cisplatin and poly(AHAEBD). This reduction in IC$_{50}$ for [Fe(poly(AHAEBD)$_2$)].Na$_3$ when contrasted with cisplatin suggests an enhanced cytotoxicity of this compound against A375 cancer cells. Moreover, in comparison to poly(AHAEBD), the polymer-complex [Fe(poly(AHAEBD)$_2$)].Na$_3$ demonstrates heightened cytotoxicity, highlighting how the formation of the polymer-complex contributes to an enhancement in cytotoxicity against melanoma cells.

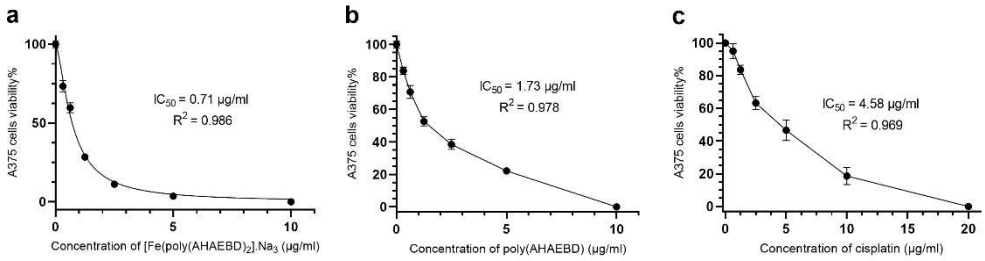

Figure 6. Cell viability% ± SD of A375 cell line after 24 h treatment with six doses of the a) [Fe(poly(AHAEBD)$_2$].Na$_3$, b) cisplatin and c) poly(AHAEBD).

Iron complexes can exert diverse effects on the cell life cycle, encompassing the stabilization or inhibition of iron absorption, disruption of iron signaling pathways, and the induction of iron free radical generation within cancer cells [32]. Elevating cellular iron levels leads to an upsurge in radical species, such as hydroxyl radicals, resulted in the fragmentation of DNA nucleotide sequences and eventual demise of cancer cells [33]. Notably, the influence of the synthesized polymer-complex stands out surpassing both cisplatin (4.58 µg/mL) as a reference and other iron complexes. For example, the IC$_{50}$ for pyridoxal-thiosemicarbazide-iron (III) and N,N'-bis[salicylidene]-1,3-diamino-1,2,2-trimethylcyclopentane-iron (III) on the A375 cancer cell line are approximately 29.79 µg/mL and 12.10 µg/mL, respectively [34,35]. The notably low IC$_{50}$ value (0.71 µg/mL) of the synthesized polymer-complex, coupled with the innovative structural design, can be regarded as a distinct advantage of this study.

4. Conclusion

The complex polymer [Fe(poly(AHAEBD)$_2$].Na$_3$ was synthesized by reacting the poly(AHAEBD) polymer with iron (III), and subsequently, its anticancer potential, along with that of poly(AHAEBD) and cisplatin as a reference, was evaluated on a A375 human malignant melanoma cells line using the MTT method. The results obtained indicate that the IC$_{50}$ value of the polymer complex [Fe(poly(AHAEBD)$_2$].Na$_3$ (0.71 µg/mL) is lower than that of cisplatin (4.58 µg/mL),

highlighting the superior efficacy of this complex-polymer against the A375 cells. Moreover, after the formation of the complex polymer, the IC_{50} value of the poly(AHAEBD) polymer (1.73 µg/mL) reduces, indicating an increase in the polymer-complex cytotoxicity and anticancer effects. The synthesized polymer demonstrates a pronounced tendency to coordination with iron ions due to its arrangement of alternating amine and hydroxy groups. Furthermore, its remarkable water solubility can enhance its reactivity with a variety of metal ions.

The noteworthy aspect of this study is its establishment of a novel path using polycationic linear polymers for synthesis of effective polymer-complexes targeting cancer cells in in-vitro experiments. Thanks to its remarkable characteristics, this polymer complex holds the potential to serve as a candidate for future in-vivo tests.

Author Contributions: Conceptualization, S.H. and E.N.; methodology, S.H.; software, S.H.; validation, S.H. and E.N.; formal analysis, S.H.; investigation, S.H.; resources, S.H.; data curation, S.H. and E.N.; writing—original draft preparation, S.H.; writing—review and editing, S.H. and E.N.; visualization, S.H. and E.N.; supervision, S.H.; project administration, S.H.; funding acquisition, S.H. All authors have read and agreed to the published version of the manuscript.

Funding: This research received no external funding.

Data Availability Statement: Data are contained within the article.

Conflicts of Interest: The authors declare no conflict of interest.

References

1. O'Neill, C.H.; Scoggins, C.R. Melanoma. J. Surg. Oncol. 2019, 120, 873-881. https://doi.org/10.1002/jso.25604.
2. Domingues, B.; Lopes, J.M.; Soares, P.; Pópulo, H. Melanoma treatment in review. Immuno Targets Ther. 2018, 7, 35-49. https://doi.org/10.2147/itt.s134842.
3. Gamberi, T.; Hanif, M. Metal-Based Complexes in Cancer Treatment. Biomedicines. 2022, 10(10), 2573. https://doi.org/10.3390/biomedicines10102573.
4. Bouché, M.; Hognon, C.; Grandemange, S. Recent advances in iron-complexes as drug candidates for cancer therapy: reactivity, mechanism of action. Dalton Trans. 2020, 49, 11451-11466. https://doi.org/10.1039/D0DT02135K.
5. Guo, Q.; Li, L.; Hou, S. The Role of Iron in Cancer Progression. Front. Oncol. 2021, 11, 778492. https://doi.org/10.3389/fonc.2021.778492.
6. Kwok, J.C.; Richardson, D.R. The iron metabolism of neoplastic cells: Alterations that facilitate proliferation? Crit. Rev. Oncol. Hematol. 2002, 42, 65–78. https://doi.org/10.1016/s1040-8428(01)00213-x.
7. Bauckman, K.; Haller, E.; Taran, N. Iron alters cell survival in a mitochondria-dependent pathway in ovarian cancer cells. Biochem. J. 2015, 466, 401–413. https://doi.org/10.1042/bj20140878.
8. Filipovic, M.R.; Koppenol, W.H. The Haber-Weiss Reaction - The Latest Revival. Free Radical Biol. Med. 2019, 145, 221–222. https://doi.org/10.1016/j.freeradbiomed.2019.09.017.
9. Lipinski, B. Hydroxyl Radical and Its Scavengers in Health and Disease. Oxid Med. Cell Longevity 2011, 809696. https://doi.org/10.1155/2011/809696.
10. Khoshmanzar, M.; Ghanbarzadeh, B.; Hamishehkar, H.; Sowti, M.; Hoseini, M. Sodium Caseinate-Carrageenan Biopolymeric Nanocomplexes as a Carrier of Vitamin D: Study of Complex Formation, Particles Size and Encapsulation Efficiency. IJPST 2014, 27(1), 37-49. https://dx.doi.org/10.22063/jipst.2014.1043.
11. Bahrani, S.; Ghanbarzadeh, B.; Hamishehkar, H.; Hoseini, M. Study of Thermal Properties, Turbidity, Effective Factors on Particle Size and Oscillatory Rheology of Pectin-Caseinate Biopolymer Nanocomplexes. IJPST 2013, 25(6), 433-447. https://dx.doi.org/10.22063/jipst.2013.852.
12. Sriwidodo, A.; Umar, K.; Wathoni, N. Liposome-polymer complex for drug delivery system and vaccine stabilization. Heliyon 2022, 8(2), e08934. https://doi.org/10.1016/j.heliyon.2022.e08934.
13. Soares, D.C.F.; Domingues, S.C.; Viana, D.B. Polymer-hybrid nanoparticles: Current advances in biomedical applications. Biomed. Pharmacother. 2020, 131, 110695. https://doi.org/10.1016/j.biopha.2020.110695.
14. Siddique, S.; Chow, J.C.L. Gold Nanoparticles for Drug Delivery and Cancer Therapy. Appl. Sci. 2020, 10, 3824. https://doi.org/10.3390/app10113824.

15. Salehipour, M.; Rezaei, S.; Mosafer, J. Recent advances in polymer-coated iron oxide nanoparticles as magnetic resonance imaging contrast agents. J. Nanopart. Res. 2021, 23, 48. https://doi.org/10.1007/s11051-021-05156-x.
16. Machado, J.F.; Correia, J.D.G.; Morais, T.S. Emerging Molecular Receptors for the Specific-Target Delivery of Ruthenium and Gold Complexes into Cancer Cells. Molecules 2021, 26, 3153. https://doi.org/10.3390/molecules26113153.
17. Kuikun, Y.; Zhiqing, Y.; Guocan, Y.; Zhihong, N.; Ruibing, W.; Xiaoyuan, C. Polyprodrug Nanomedicines: An Emerging Paradigm for Cancer Therapy. Adv. Mater. 2022, 34. https://doi.org/10.1002/adma.202107434.
18. Inamura, I.; Inamura, K.; Jinbo, Y.; Miharad, T.; Sasaoka, Y. Preparation of metal phthalocyanine (MPc)–polymer complexes: the possible anti-cancer properties of FePc–polymer complexes. Heliyon 2019, 5(3), e01383. https://doi.org/10.1016/j.heliyon.2019.e01383.
19. Corra, S.; Curcio, M.; Baroncini, M. Photoactivated Artificial Molecular Machines that Can Perform Tasks. Adv. Mater. 2020, 32(20), 1906064. https://doi.org/10.1002/adma.201906064.
20. Satan, A.B.; Patsula, V.; Dydowiczová, A.; Gunár, K.; Velychkivska, N.; Hromádková, J.; Petrovský, E.; Horák, D. Cationic Polymer-Coated Magnetic Nanoparticles with Antibacterial Properties: Synthesis and In Vitro Characterization. Antibiotics 2022, 10, 1077. https://doi.org/10.3390/antibiotics10091077.
21. Gröning, A.; Ahrens, H.; Ortmann, T.; Lawrenz, F.; Helm, C.A. Polyetylenimine (PEI) adsorption to a DMPG lipid-monolayer in the presence of iron salts and EDTA. Polymer 2016, 102, 386-395. https://doi.org/10.1016/j.polymer.2016.08.034.
22. Sari, N.; Kahraman, E.; Sari, B.; Özgün, A. Synthesis of Some Polymer-Metal Complexes and Elucidation of their Structures. J. Macromol. Sci., Part A 2006, 43(8), 1227-1235. https://doi.org/10.1080/10601320600737484.
23. Wanga, Z.; Tsarevsk, N.V. Well-Defined Polymers Containing a Single Mid-Chain Viologen Group: Synthesis, Environment-Sensitive Fluorescence, and Redox Activity. Polym. Chem. 2016, 7, 4402-4410. https://doi.org/10.1039/C6PY00628K.
24. Garkusha-Bozhko, V.S.; Shvaika, O.P. Reaction of pyridines with epichlorohydrin. Chem. Heterocycl. Compd. 1990, 26, 434-437. https://doi.org/10.1007/BF00497217.
25. Mehdipour, E.; Hasanvandi, S.; Shafieyoon, P. Synthesis, characterization and cytotoxicity investigation of juglone palladium complex; theoretical and biological properties of juglone as an employed ligand. J. Iran. Chem. Soc. 2022, 19, 3387-3395. https://doi.org/10.1007/s13738-022-02532-9.
26. Zhu, D.; Li, W.; Wen, H.M. Self-assembled Mn-doped ZnSe quantum dot–methyl viologen nanohybrids as an OFF–ON fluorescent probe for time-resolved fluorescence detection of tiopronin. Anal. Methods 2013, 5, 4321-4324. https://doi.org/10.1039/C3AY40907D.
27. Ju, H.; Duan, J.; Lu, H. Cross-Linking with Diamine Monomers to Prepare Composite, A single rapid route for the synthesis of reduced graphene oxide with antibacterial activities. Chem. Mater. 2014, 26, 2983-2990. https://doi.org/10.3389/fchem.2021.7793.
28. Hayami, R.; Nakamoto, W.; Sato, Y. Organic–inorganic hybrids based on poly(bisphenol A-co-epichlorohydrin) containing titanium phosphonate clusters. Polym. J. 2019, 51, 1265-1271. https://doi.org/10.1038/s41428-019-0243-y.
29. Oliveira, T.D.; Cabeza, N.A.; Silva, G.T.S.T. Coordination of the natural ligand lapachol to iron(II): synthesis, theoretical study and antiproliferative activity. Transit. Met. Chem. 2021, 46, 111-120. https://doi.org/10.1007/s11243-020-00427-3.
30. Garbutcheon-Singh, K.B.; Galanski, M.; Keppler, B.K. Synthesis, characterisation and cytotoxicity of [(1,10-phenanthroline)(1R,2R,4R/1S,2S,4S)-4-methyl-1,2-cyclohexanediamine)platinum(II)]2+ (PHEN-4-MeDACH). Inorg. Chim. Acta 2016, 152, 441. https://doi.org/10.1016/j.ica.2015.10.048.
31. Mirmalek, S.A.; Azizi, M.A.; Jangholi, E.; Damavandi, S.Y.; Javidi, M.A.; Parsa, Y.; Parsa, T.; Salimi Tabatabaee, S.A.; Ghasemzadeh kolagar, H.; Alizadeh Navae, R. Cytotoxic and apoptogenic effect of hypericin, the bioactive component of Hypericum perforatum on the MCF-7 human breast cancer cell line. Cancer Cell Int. 2016, 16, 3. https://doi.org/10.1186/s12935-016-0279-4.
32. Jung, M.; Mertens, C.; Tomat, E.; Brüne, B. Iron as a Central Player and Promising Target in Cancer Progression. Int. J. Mol. Sci. 2019, 20, 273. https://doi.org/10.3390/ijms20020273.
33. Tifoun, N.; De Las Heras M, J.M.; Guillaume, A.; Bouleau, S.; Mignotte, B.; Le Floch, N. Insights Into the Roles of the Sideroflexins/SLC56 Family in Iron Homeostasis and Iron-Sulfur Biogenesis. Biomedicines 2021, 9(2), 103. https://doi.org/10.3390/biomedicines9020103.

34. Jevtovic, V.; Alshamari, A.K.; Milenković, D.; Dimitrić Marković, J.; Marković, Z.; Dimić, D. The Effect of Metal Ions (Fe, Co, Ni, and Cu) on the Molecular-Structural, Protein Binding, and Cytotoxic Properties of Metal Pyridoxal-Thiosemicarbazone Complexes. Int. J. Mol. Sci. 2023, 24(15), 11910. https://doi.org/10.3390/ijms241511910. PMID: 37569285; PMCID: PMC10419307.
35. Murtinho, D.; da Rocha, Z.N.; Pires, A.S.; Jiménez, R.P.; Abrantes, A.M.; Laranjo, M.; Mamede, A.C.; Casalta-Lopes, J.E.; Botelho, M.F.; Pais, A.A.C.C.; Nunes, S.C.C.; Burrows, H.D.; Costa, T.; Silva Serra, M.E. Synthesis, characterization and assessment of the cytotoxic activity of Cu(II), Fe(III) and Mn(III) complexes of camphoric acid-derived salen ligands. Appl. Organometal. Chem. 2015, 29(7), 425-432. https://doi.org/10.1002/aoc.3309.